Int J Fract (2017) 203:263–276
DOI 10.1007/s10704-016-0145-3

COMPMECH

Numeral modeling of fracture failure of recycled aggregate concrete beams under high loading rates

K. Musiket · F. Vernerey · Y. Xi

Received: 10 April 2016 / Accepted: 8 August 2016 / Published online: 27 September 2016

Abstract Fracture tests of recycled aggregate concrete (RAC) beams of different sizes were conducted under high loading rates. In order to characterize the effect of high loading rate on the behavior of RAC beams, two new material models were used together with the commercial finite element software ABAQUS^{R}. One model is a viscoelastic model that can predict the increase of stiffness (modulus of elasticity) of RAC with increasing loading rate, and the other model is a multiphase composite model that can determine the effective stiffness of RAC taking into account the special internal structure of recycled aggregate. Two different cases were considered in the numerical simulation. Case 1 is for fixed beam size under different loading rates, and Case 2 is for fixed loading rate with different beam sizes. For Case 1, the simulation results of the maximum loads under three different strain rates agreed with test data quite well. The Force-CMOD curves of the numerical simulation and test data showed similar trends. The higher the strain rates, the wider the high stresses spread in the crack propagation zone. The good agreements with the test data indicated that the two new material models can characterize the effect of high loading rate on RAC beams very well. For Case 2, three beam sizes and one loading rate was studied. The post-peak Force versus CMOD curves from the simulation follow the same trend of the test data. The stress distributions in the beams of different sizes are similar. On the other hand, the maximum loads predicted by the numerical model did not agree very well with test data. This is due to the fact that the maximum forces of RAC notched beams exhibited size effect, which was not considered in the fracture criteria adopted in ABAQUS^{R} and not in the two new material models. This will be a topic for future research.

Keywords Recycled aggregate concrete · Fracture in beams · Viscoelastic model · Composite model · High loading rate · Size effect

1 Introduction

The large amount of consumption of coarse aggregate in the construction industry for reinforced concrete structures is not sustainable due to the limited resource of natural stone. There is a pressing need to use recycled aggregate from demolished concrete structures to make recycled aggregate concrete (RAC). RAC can be used as a potential structural material in the construction of concrete structural members, such as beams and columns. However, the application of RAC as a structural material has been hindered because of several rea-

K. Musiket · F. Vernerey · Y. Xi (✉)
University of Colorado at Boulder, Boulder, CO, USA
e-mail: yunping.xi@colorado.edu

K. Musiket
Department of Civil Engineering, Faculty of Engineering, Rajamangala University of Technology Thanyaburi, 39 Moo1, Rangsit-Nakhonnayok Rd. Klong6, Thanyaburi, Pathumthani 12110, Thailand
e-mail: kamtornkiat.m@en.rmutt.ac.th

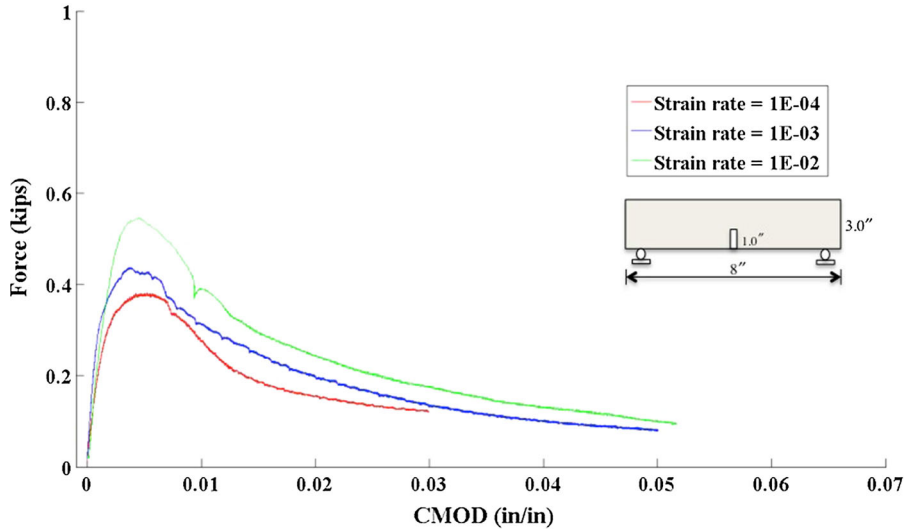

Fig. 1 Force versus CMOD curves of RAC beams at different strain rates (Musiket et al. 2016)

sons, such as the higher cost of RAC (due mainly to processing) comparing with regular concrete and the lack of design codes for the structures made of RAC. More importantly, the mechanical properties of RAC are different from those of regular concrete, and they have not been understood very well. Recycled aggregate has a layer of residual cement paste on its surface, which leads to a weak bond between the aggregate and the surrounding new cement paste, and the lower bond may result in a lower compressive strength. Several methods have been developed to process recycled aggregates in order to improve the interface bond, including surface pretreatment of recycled aggregate using various types of coatings (Liang et al. 2013).

Fracture property of RAC members under high loading rates is one of the mechanical properties that have not been understood well. In general, mechanical properties such as strength and stiffness of RAC increases with increasing loading rate, the same as the mechanical properties of regular concrete under a high loading rate. However, some of the fracture behaviors of RAC under high loading rates are different from those of regular concrete (Musiket et al. 2016). One can see from Fig. 1 that the maximum loads for the beams under different loading rates are different, and the maximum load increases with increasing loading rate. Based on the test data, the fracture properties of RAC beams were obtained and found to be rate-dependent. The critical stress intensity factor, K_{Ic}, and the fracture energy release rate, G_f, increase with increasing loading rate. However, the RAC beams were found to be less brittle than under the static load. This was evidenced by the effective fracture process zone size, c_f, which increases with increasing loading rate.

There has been no numerical modeling developed to simulate fracture properties of RAC structural members such as beams under different loading rates. Two material models have been developed for RAC based on compression test data of RAC cylinders. The material models have not been examined by other loading configurations and other structural shapes and sizes. The motivation of this paper is to carry out a numerical modeling of the fracture failure of RAC beams under high loading rates using the recently developed material models. The numerical simulation will be verified by recent experimental results of RAC beams. The paper will be organized as follows. Fundamental models for analyzing fracture processes of concrete will be described first, which were developed for regular concrete and will be used for the fracture analysis of recycled aggregate concrete. Basic concepts of eXtended Finite Element Method (XFEM) for crack propagation in concrete materials and the fracture analysis criteria in the commercial finite element software ABAQUS^R will be introduced. Two new material models taken into account the loading rate effect and composition effect for RAC will be described. Finally, a numerical simulation of notched-beams made of RAC will be conducted using the new material models and ABAQUS^R. The numerical results will be compared with the test data of Musiket et al. (2016).

2 Fracture analysis of regular concrete materials

In general, fracture mechanics in heterogeneous media typically involve two distinct and separate length-scales. On the one hand, crack nucleation and growth occurs via the evolution of damage ahead of the crack tip, in a relatively small region, known as the process zone. In this region, materials usually exhibit a complex response such as micro-cracking, particle debonding and eventually a strain-softening response that may induce size effects. A micromechanical modeling approach is often necessary to accurately capture these mechanisms and their effects on fracture resistance. On the other hand, fracture initiation and propagation highly depends on macroscopic loading, geometry and macroscopic material features. At this level, a continuum description is usually preferred due to its ability to describe uniform material deformation and its low computational cost. This has motivated the development of multiscale methods based on size-dependent continuum descriptions for damage description and softening (Vernerey et al. 2008a, b) or that include an explicit crack and corresponding singular fields as part of the formulation. The latter approach as led to the popular extended finite element method XFEM (Moës et al. 1999) that proved highly efficient and convenient to study crack propagation in brittle and quasi-brittle materials such as concrete. To better understand the role of microstructure and materials failure, computational multiscale methods have further been developed in order to bridge microstructural material descriptions (in regions in which highly heterogeneous deformation occurs) and the continuum description (where the deformation field is homogeneous). For instance, the bridging scale method (Wagner and Liu 2003) was first used to bridge continuum and atomistic fracture by overlapping a fine scale description at the crack tip with a coarse scale finite element mesh. This method was later combined with adaptive methods, such as the ACM^2 (Vernerey and Kabiri 2014a, b) and VCFEM (Ghosh et al. 2001; Raghavan and Ghosh 2007), so that an automatic refined material description could be provided near the tip of propagating cracks. Such methods were coupled with meshless methods (Rabczuk and Belytschko 2007; Rabczuk et al. 2009, 2010; Zhuang et al. 2014) for smoother approximation and the avoidance of mesh distortion near the crack tip.

In particular, the heterogeneous feature of internal structure of regular concrete requires some specific attention. To this end, the models used for fracture analysis of regular concrete under static loading are introduced first in this section. The new model for recycled aggregate concrete under high loading rate will be described later.

Upon the pioneering work of Hillerborg et al. (1976), the development of fictitious crack model based on a cohesive crack model for the crack propagation of concrete, a number of fracture models have been proposed and employed to verify the nonlinear fracture behavior of concrete structures. These are: the crack band model (Bazant and Oh 1983), the two-parameter fracture model (Jenq and Shah 1985), the size-effect method (Bazant 1984), the effective crack model (Nallathambi and Karihaloo 1986), and the K_R-curve method based on Cohesive force (Xu and Reinhardt 1998). Among these models, the cohesive crack and crack band model can be used for numerical methods such as finite element or boundary element, while the other models are analytical models. The cohesive crack model and the crack band model will be introduced in the following and the other models will not be covered.

2.1 Cohesive crack model (CCM) or fictitious crack model (FCM)

Hillerborg et al. (1976) initially applied a fictitious crack model to simulate the softening damage of concrete structures. They confirmed that the crack formation and propagation and failure analysis can be performed with a cohesive crack model even when coarse mesh is used. Subsequently, the cohesive crack method has been modified and used by many researchers over a long period of time. The fictitious crack model was extended into finite element code to simulate mixed-mode crack analysis using six-node interface elements. Barker et al. (1985) was the first who concluded that the LEFM method was not suitable to predict unstable cracks in concrete. The process zone length in concrete and fiber reinforced concrete is not a material property by conventional sense but depends on the specimen size and loading configurations.

The cohesive zone model is a uniaxial method which considers a zero width of process zone and is not quite suitable for large-scale analysis. In contrast, it is a good approximation of the real physical process zone. The essential basis of this model still has the ability to describe the nonlinear behavior at the crack tip and

around its vicinity. There are a number of applications in recent time including who applied the model on a wedge splitting test to compare load-crack mouth opening displacement (P-CMOD) between finite element and experimental results for the characterization of bilinear softening law. Recently, Roesler et al. (2007) developed the finite element cohesive zone mode using bilinear softening to predict the monotonic loading of three-point bending test with various sizes and compared the results with experimental results for fracture properties.

Zhao et al. (2007) demonstrated the experimental results for a three-point bending test notched-beam and wedge-splitting test with different mixes designed to investigate the effect of both size and geometry on fracture parameters. It was observed that the fracture energy increases with an increase in specimen size for both the specimen geometries. Elices et al. (2009) performed a fracture test on different types of concrete made with three types of spherical aggregates and two kinds of matrix interface to investigate the influence of matrix-aggregate interface and aggregate strength of softening curve, using the fictitious crack model with bilinear softening curve. The highest specific fracture energy values were determined with strong aggregates well bonded to the matrix because the crack path avoids the aggregates and wanders through the matrix resulting in the increased value of the fracture area. The critical crack opening value appeared to be almost insensitive to the type of interface and matrix of concrete in the case of strong aggregates being used, whereas this opening was larger than the corresponding matrix in the case of weak aggregates.

2.2 Crack band model (CBM)

Bazant and Oh (1983) developed the crack band model in which the fracture process zone is operated as a system of parallel cracks distributed in finite element. Material behavior is characterized by $\sigma - \epsilon$ response. The width of the fracture process zone length, h_c, is assumed to be a material constant which can be determined from the experiment. It is usually assumed to be three times the aggregate size for normal concrete to ensure mesh insensitivity of the model. In this model, crack band is modeled by changing the isotropic elastic moduli to an orthotropic, subsequently reducing the stiffness in a normal direction to the cracking plane.

The crack band model suffers from many limitations such as (1) refinement of the mesh size cannot be smaller than the cracking zone width, (2) the zigzag crack band propagation needs special mathematical treatment, (3) a typical square mesh introduces a certain degree of directional bias, and (4) possible variations of the cracking width and hence fracture energy cannot be taken into account.

3 Fracture criteria in ABAQUS

ABAQUS^R was used in the present study for fracture analysis of RAC beams under high loading rate. The basic fracture criteria used in ABAQUS^R under static loading will be introduced in this section. There are some materials models available in ABAQUS^R that can handle high loading rate effect. However, those models were not developed for recycled aggregate concrete. Therefore, new material models will be described in the next section for recycled aggregate concrete under high loading rate. The new models will be used together with ABAQUS^R for the numerical analysis.

ABAQUS^R provides two approaches to study crack initiation and propagation using XFEM. The first one is based on Traction-separation Cohesive Behavior. This is the general interaction modeling capability which can be used for brittle or ductile materials. This XFEM-based method can be used to simulate discontinuities along an arbitrary, dependent path in solid, since a crack propagation is not coincided to the element's mesh. In this case, a near crack-tip singularity is unnecessarily needed. The only jump in the displacement across a cracked element is taken into account. Fictitious nodes will be introduced to represent the discontinuity of the crack or surface elements. At the beginning, each fictious node is coincident to its adjacent nodes. When an element is cut by the cracks, the element will be separated into two parts. Each part is consisted of normal and fictitious nodes depending on the orientation of the cracks or surfaces. The separation is controlled by the cohesive law until the cohesive strength of the elements is equal to zero, then the phantom and real nodes move freely. This made an effective and attractive engineering approach and was used for multiple cracks in solids. It has been proven that there is almost no mesh dependence if the mesh is fine (Song et al. 2006).

The second approach is based on the principles of Linear Elastic Fracture Mechanics (LEFM). It is more

suitable for brittle crack propagation problems. Similar to the XFEM-based cohesive segments method described above, only displacement jump across the enriched elements is considered. Therefore, the crack has to propagate across the entire element. The strain energy release rate near the crack tip is determined using the modified Virtual Crack Closure Technique (VCCT). In this method, the real nodes and fictitious nodes will be separated when the equivalent strain energy release rate exceeds the critical strain energy release rate at the crack tip of an enriched element. The traction will be linearly decreased all over the separation between two surfaces.

There are six failure criteria provided in ABAQUS^R depending on the type of analysis, either the standard or explicit analysis. Crack propagation analysis is carried out on a nodal basis. The crack-tip nodes separate when fracture criterion reaches the value 1.0 within a given tolerance. Since the VCCT technique is available for both implicit and explicit schemes, it is the most interest criterion for this study.

The Virtual Crack Closure Technique (VCCT) uses the concept from linear elastic fracture mechanics (LEFM), therefore it is more appropriate for brittle material problems which crack propagation propagates through pre-existing surfaces. The assumption of VCCT criterion is that there are the same amount of the strain energy which releases when crack is initiated and strain energy which requires to close that crack.

ABAQUS^R also provides user-defined user subroutine UDMGINI damage initiation criterion to handle the user specular materials. User can define many damage criteria, $f_{indexi}, i = 1, 2, 3, \ldots$, but the actual damage for enriched elements will be governed by the most severe one. All criteria are in a form of the ratio between current state parameters, stress, strain, etc., and the maximum allowable of corresponding values.

For this study, the cohesive element method was used as the failure criterion. The maximum principal stress criterion was applied for damage initiation procedure based on maximum principal stress calculated from the fracture test conducted under different loading rates (Musiket et al. 2016).

4 The new material models for RAC under high loading rates

The material models available in ABAQUS^R do not consider the special features of recycled aggregates used in RAC. In the literature there are numerical simulation models developed for regular concrete under high loading rates (Rabczuk and Eibl 2003, 2006), but not for RAC. Therefore, two new material models for RAC under high loading rates were developed by a systematical experimental study and a comprehensive theoretical analysis (see the Ph.D. dissertation by Dr. Musiket at University of Colorado at Boulder, 2014). One model is for the rate effect, and the details of the model development can be seen in Musiket et al. (2016). The other is for the special internal structure of recycled aggregate, called composition effect, and the details of the model development can be seen in Musiket et al. (2016). For reader's convenience, the following is a brief description of the two new models.

4.1 Viscoelastic model for high strain rate effect of RAC

For the rate effect, various viscoelastic models were commonly used for slow (long-term) loading effect on stiffness of viscoelastic materials, such as creep effect on modulus of elasticity of concrete (Bazant and Xi 1995). In the new viscoelastic model for recycled aggregate, we used Prony series (also called generalized Maxwell model) for stiffness of RAC under high loading rates. Calibrated by experimental data of RAC cylinders under various high loading rates, the following viscoelastic model was developed for modulus of elasticity of RAC under high loading rates.

$$E(\dot{\epsilon}) = R_{\dot{\epsilon}}^{V} = E_{end}/E_0 + \sum_{i=1}^{n}(E_i/E_0)e^{-(r)/r_i} \qquad (1)$$

in which $E_i/E_0 = e_i$ are the normalized Prony parameters, which are shown in Table 1; E_0 and E_{end} are the elastic moduli under the slowest and fastest loading rate, which are also shown in Table 1; and τ and τ_i are the applied strain rate and the selected strain rates under consideration (the first column in Table 1). Figure 2 shows the comparison of predicted and test data of elastic moduli of RAC under high loading rates.

4.2 Generalized multiphase self-consistent model stiffness for RAC

The use of recycled aggregate in concrete will lead to low compressive strength and low stiffness. As mentioned in the introduction, several methods have been

Table 1 The Prony parameters (the last column) for the viscoelastic model of RAC

Strain rate (/s)	E_0 (*literature*) (Mpa)	E_0 (*predicted*) (Mpa)	% Diff	Normalized prony (e_i)
0.001	25,600	25,809.90	0.4178	0.0207
0.01	26,700	26,377.83	0.4743	0.0027
0.1	28,753	28,163.31	−2.3260	0.0756
1.0	31,469	31,705.96	−0.7530	0.1617
10	34,166	34,960.72	2.0508	0.1421
100	36,582	36,408.48	1.2065	0.0290
1000	37,000	36,845.40	−0.8199	0.0216

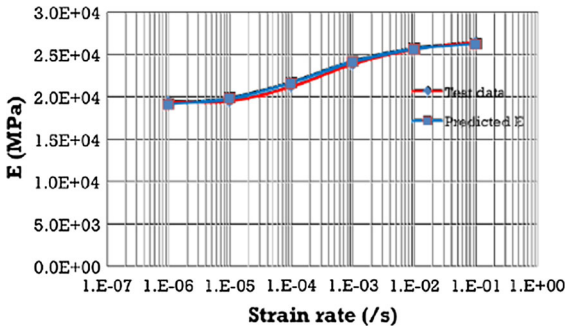

Fig. 2 Comparison of predicted and test data (Musiket 2014) of elastic moduli of RAC under high loading rates

developed to improve mechanical properties of RAC, including pretreatment of the surface of recycled aggregates. With the help of pretreatment techniques developed in previous studies (Liang et al. 2013; Musiket et al. 2016), the compressive strength of recycled aggregate concrete can reach the same level as regular concrete. However, the RAC made of recycled aggregates with surface pretreatment has a special internal structure that is different from regular concrete. Each aggregate is covered by a layer of residual cement paste, a layer of surface pretreatment material, and a layer of new cement paste. The new constitutive models take into account this special feature of multiple layered internal structure of recycled aggregate. This model was developed originally for characterization of drying shrinkage and bulk modulus of concrete (Xi and Jennings 1997). It was used in this study for characterization of modulus of elasticity of RAC. Recycled aggregate concrete was considered as a composite material as shown in Fig. 3. The internal structure of RAC can be simplified as many geometrically similar elements with different sizes. Each element is composed of concentric spheres with multiple layers as shown in Fig. 4.

The components (the layers) in the basic element are: (1) natural aggregate as the core, (2) old residual mortar on the surface of the core, (3) new mortar from surface pretreatment to enhance the bond between the old residual mortar and the new mortar, and (4) new mortar from final mix procedure.

For recycled aggregate, the volume fractions of the four constituent phases are not constants but functions of time depending on the concrete mix designs used for the new concrete as well as for the residual mortar (the old concrete). The mechanical properties of the four phases depend on the degree of hydration reactions of the new and old cements used in a RAC, and thus on time. As a result, the effective modulus of RAC is also a function of time.

A generalized n-phase composite model was developed by Xi and Jennings (1997) for bulk modulus of concrete. Assuming the Poisson's ratios of the constituent phases in recycled aggregates are constants, a similar model can be obtained for effective modulus of elasticity of RAC. This effective model is

$$E_{eff}^{ijk,\ldots,n} = E_n \left[1 + \frac{C_m}{\left(\frac{1-C_m}{3}\right) + \left(\frac{E_n}{E_{ijk,\ldots,n} - E_n}\right)} \right] \quad (2)$$

$$C_m = \left\{ \begin{array}{ll} \frac{\sum_{m=1}^{n-1} \phi_m}{\sum_{m=1}^{n} \phi_m} & \text{if } m \neq n \\ 1 - \phi_m & \text{if } m = n \end{array} \right\} \quad (3)$$

where $E_{eff}^{ijk,\ldots,n}$ is the effective modulus of n-phase composite; E_i are the modulus of ith component; and $E_{ijk\ldots n}$ is the modulus of $n-1$ phase composite (see details later); and C_m and C_{ij} are the volume fractions of the layers and the core.

In this study, n = 4, which is based on the basic element shown in Fig. 4. In Eq. (3) for the composite effect, $E_{ijk,\ldots,n}$ is a recursive equation as shown below when n = 4:

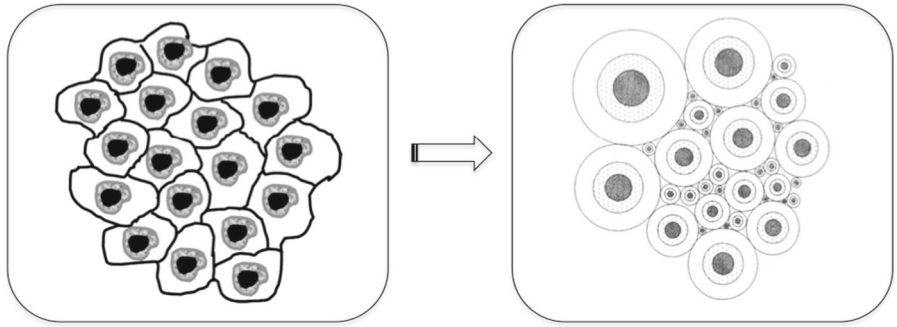

Fig. 3 The multiphase model for internal structure of recycled aggregates

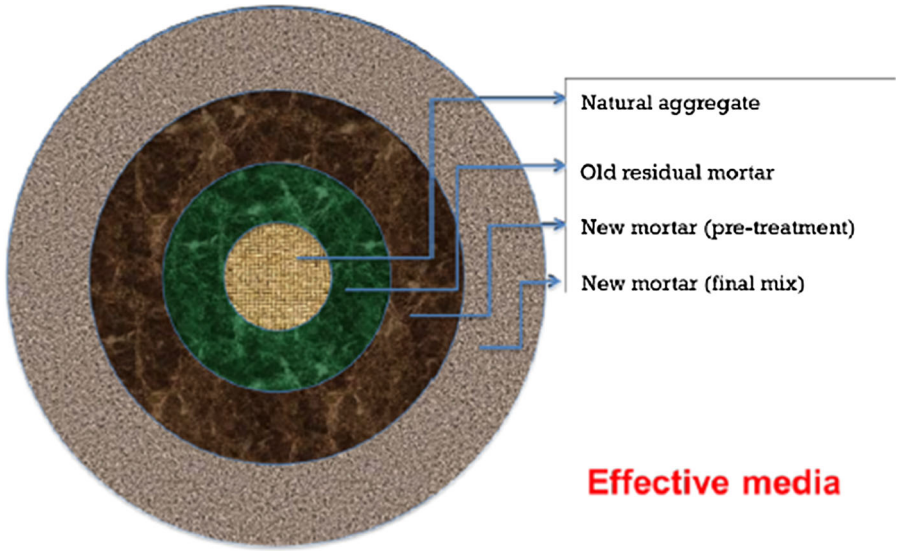

Fig. 4 The internal structure of concentric spherical element in the multiphase model

$$E_{12} = E_2\left[1 + \frac{C_{12}}{\left(\frac{1-C_{12}}{3}\right) + \left(\frac{E_2}{E_1 - E_2}\right)}\right] \tag{4}$$

$$E_{123} = E_3\left[1 + \frac{C_{23}}{\left(\frac{1-C_{23}}{3}\right) + \left(\frac{E_3}{E_{12} - E_3}\right)}\right] \tag{5}$$

$$E_{1234} = E_4\left[1 + \frac{C_{34}}{\left(\frac{1-C_{34}}{3}\right) + \left(\frac{E_4}{E_{123} - E_4}\right)}\right] \tag{6}$$

4.3 The combined model: strain rate multiphase model (SRMM)

The combination of the two new theoretical models enables us to predict the stiffness of composite materials considering both the constituent phases and loading rates. This combined theoretical model may be called "Strain Rate Multiphase Model (SRMM)" (Musiket 2014), and it is shown in the following equation:

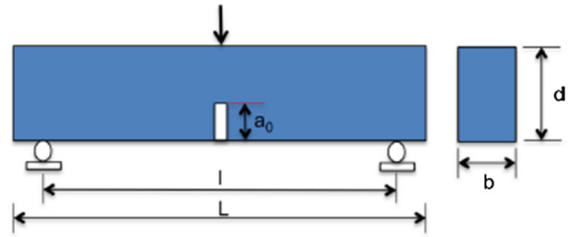

Fig. 5 Geometry of RAC beams

$$E_{(\dot{\epsilon})} = E^M_{eff} R^V_{\dot{\epsilon}} = E_n\left[1 + \frac{C_m}{\left(\frac{1-C_m}{3}\right) + \left(\frac{E_n}{E_{ijk,\ldots,n} - E_n}\right)}\right] \times \left[\frac{E_{end}}{E_0} + \sum_{i=1}^{n} \frac{E_i}{E_0} e^{-\frac{\dot{\epsilon}_i}{\dot{\epsilon}}}\right] \tag{7}$$

in which the first bracket on the right hand side represents the multiphase composite model for the internal structure of recycled aggregate as shown in Figs. 3

Table 2 Dimension of RAC beams

Size	d (m)	L (m)	I (m)	a_0(m)	b(m)	Vol (m^3)
1	0.0381	0.1016	0.0952	00.0127	0.0508	0.0002
2	0.0762	0.2032	0.1905	0.0254	0.0508	0.0007
3	0.1524	0.4064	0.3810	0.0508	0.0508	0.0031
4	0.3048	0.8128	0.7620	0.1016	0.0508	0.0125

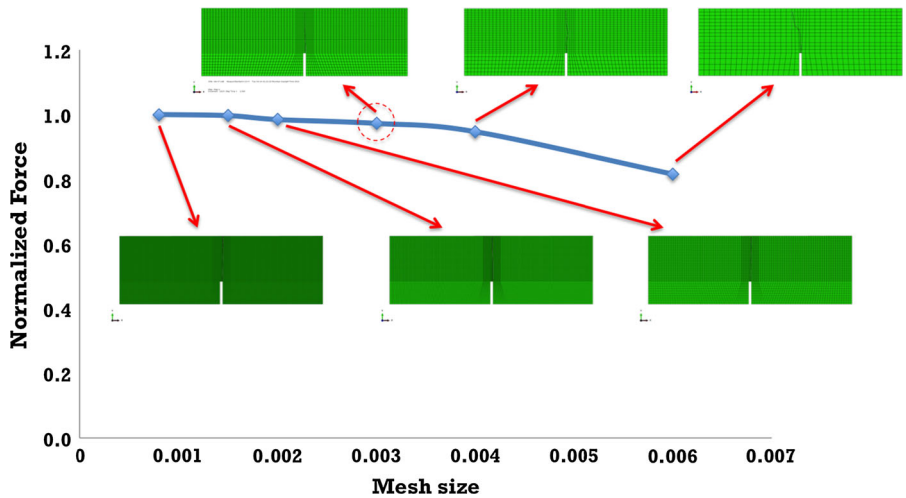

Fig. 6 Mesh size selection

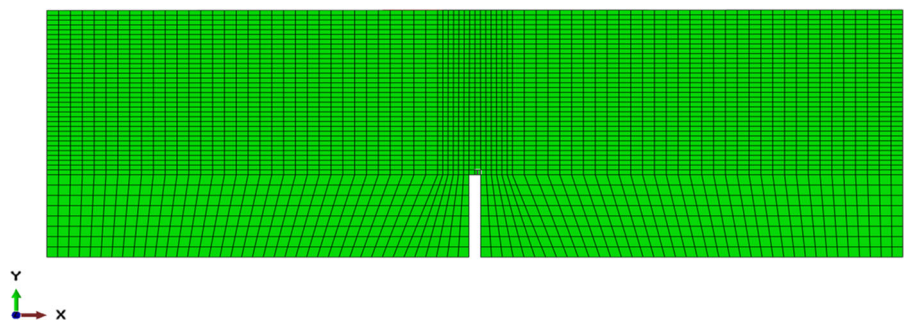

Fig. 7 2D mesh for the notched beam

and 4, and the second bracket the viscoelastic model for high loading rate.

5 Numerical simulation of RAC notched-beams

Some assumptions were used in the present study: (1) A two-dimensional plane stress model was used for RAC beams for the sake of simplicity, (2) The constitutive model, the Strain Rate Multiphase Model described in the previous section was used for RAC under high loading rates, (3) Crack propagation and damage criteria were selected from appropriate criteria provided by ABAQUS^R. A two-dimension notched-beam model with three different sizes was used in the present study

Table 3 Input parameters for the numerical simulation

Strain rate ($^{-1}$)	E^{SRMM} (ksi)	G_f (kips/in)	$\sqrt{K_{Ic}}$ (kips/in)
0.0001	2866	0.07	1.21
0.001	3230	0.08	1.29
0.01	3455	0.12	1.70

(Musiket et al. 2016). The geometry and dimensions of the beams are shown in Fig. 5 and Table 2.

The first task was to select an appropriate mesh size for optimization of both computational time and convergence. Since crack propagation analysis using XFEM is a path-dependent problem, meshing algo-

Table 4 Two different cases comparing the results simulation with test data

Size	Strain rate = 10^{-4}		Strain rate = 10^{-3}		Strain rate = 10^{-2}	
	P_u (kips)	P_u (kN)	P_u (kips)	P_u (kN)	P_u (kips)	P_u (kN)
1	0.26	1.045	0.32	1.18	**0.37**	1.33
2	0.38	1.65	0.43	1.91	**0.54**	2.23
3	**0.58**	2.35	**0.76**	2.8	**0.91**	3.6

The significance of bold values are used to compare

Table 5 Comparison of ultimate load for case 1: fixed beam size under different loading rates

Strain rate (/s)	Fu, ^{test}(kips)	Fu, ^{Abaqus}(kips)
0.0001	0.53	0.61
0.001	0.63	0.79
0.01	0.91	0.98

Table 6 Comparison of ultimate load for case 2: fixed loading rate for different beam sizes

Strain rate (/s)	Fu, ^{test}(kips)			Fu, ^{Abaqus}(kips)		
	Size 1	Size 2	Size 3	Size 1	Size 2	Size 3
0.01	0.37	0.55	0.91	0.25	0.47	0.98

rithms plays an important role. ABAQUS^{R}provides three different techniques for meshing: free, structured, and sweep, respectively. Although free meshing techniques allow us more flexibility in controlling mesh for more complex structure, it was much easier and yet more accurate to use structured meshing in this study. Six different mesh sizes were chosen to determine the relationship between mesh size and convergence. The best mesh size taking into account both computational time and mesh-independence is the red-dot circle shown in Fig. 6.

A two-dimensional notched-beam is composed of 3344 elements and 3345 nodes as shown in Fig. 7. The width of middle region in the model, 10 times of notch width, was modelled as enriched elements since crack propagation would take place within this area. A four-node quadrilateral plain stress element with reduced integration was used for the entire model due to the limitation of using XFEM for two-dimensional problems. The modulus of elasticity of RAC was determined by the new model SRMM. Poisson's ratio and density of RAC for this study are 0.25 and 2400 kg/m^3, respectively.

ABAQUS^{R}dynamic implicit scheme was used primarily for the simulation. At some higher strain rates the static standard scheme was used instead to overcome convergence issues. A cohesive-based element using VCCT technique as introduced earlier was selected for crack propagation criteria. Damage initiation criterion employed for this simulation is the maximum principal stress. Hard contact was used in surface behavior for entire enriched elements. The energy-based mixed mode based on power law fracture criterion has been chosen for damage evolution. Velocity boundary conditions, 0.0001, 0.001, and 0.01 in/s, were imposed at the top mid-span to simulate the applied loads, which are equivalent to the strain rates used in the experiment (Musiket et al. 2016). The other relevant material data are summarized in Table 3.

6 Results and discussions

The numerical study focused on two cases:

Case 1: Fixed beam size under different loading rates. In this case, the notched-beam size 3 in Table 2 was used together with a variation of strain

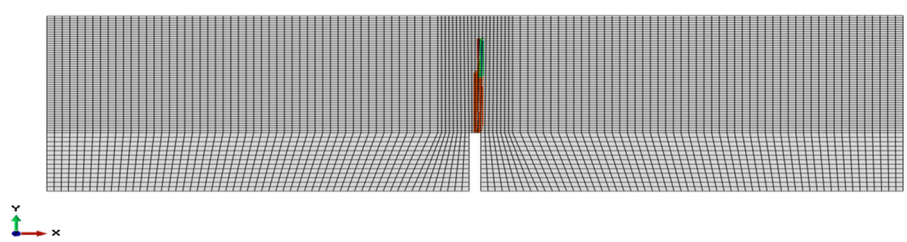

Fig. 8 Cracked elements during a crack propagation in a RAC beam

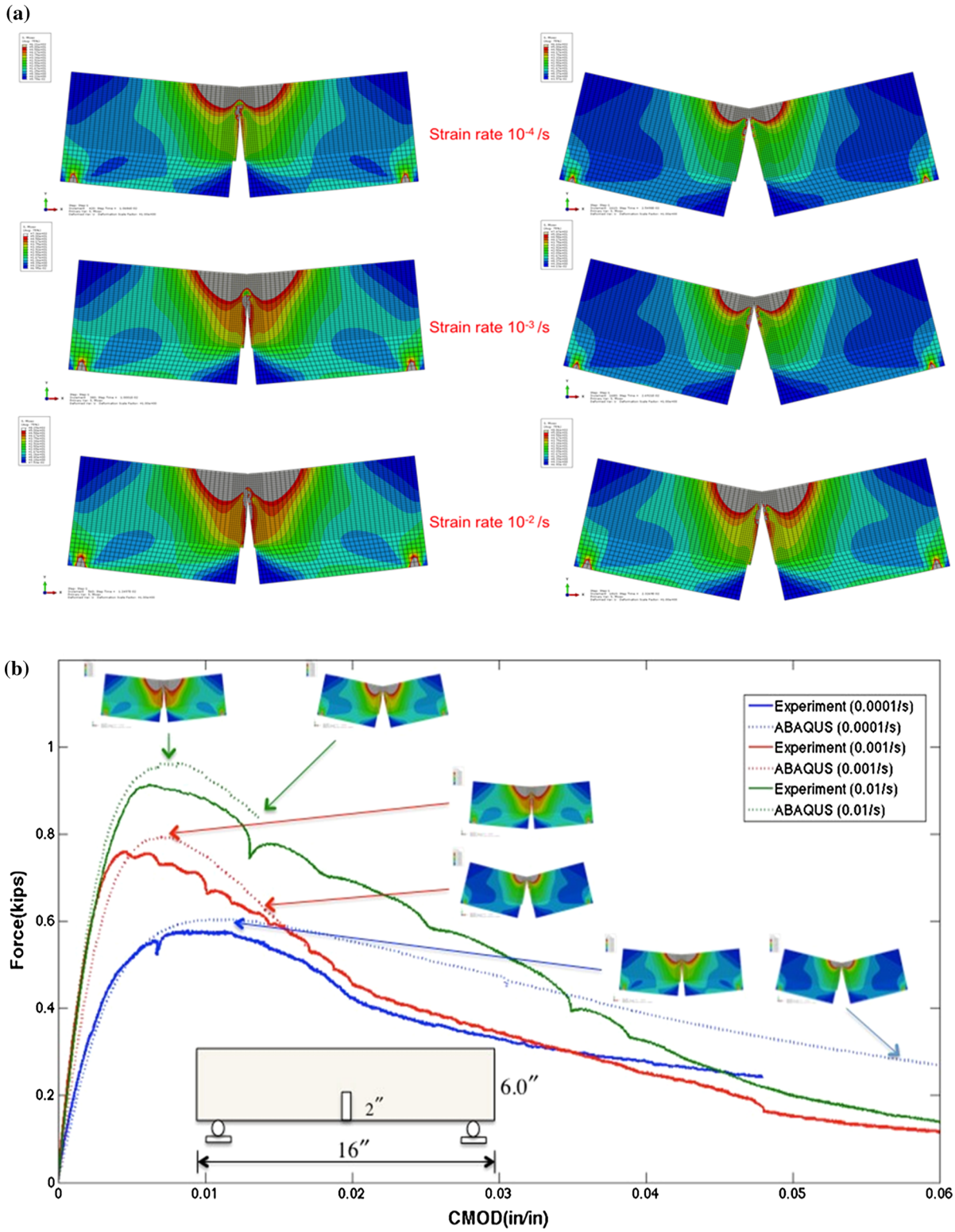

Fig. 9 Force versus CMOD and stress distributions for Case 1: fixed beam size under three different loading rates, **a** Stress distributions at peak loads (*left*) and final deformed stages (*right*) for Case 1, **b** Full force versus CMOD curves for Case 1

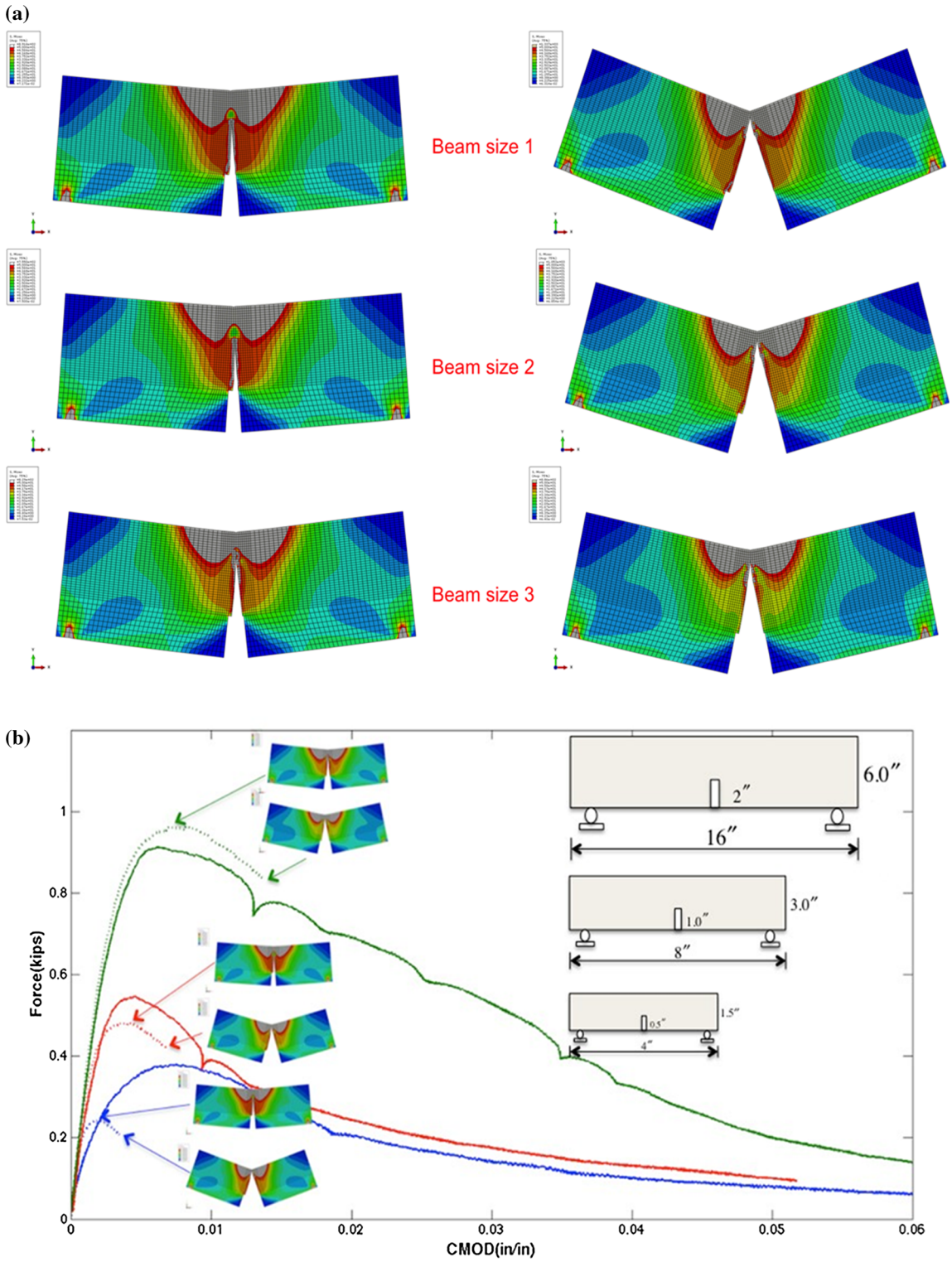

Fig. 10 Force versus CMOD and stress distributions for Case 2: fixed loading rate for three different beam sizes, **a** Stress distributions at peak loads (*left*) and final deformed stages (*right*) for Case 2, **b** Full force versus CMOD curves for Case 2

rates from $10^{-4}/s$ to $10^{-2}/s$. This case is to show the effect of loading rate on fracture properties of RAC beams.

Case 2: Fixed loading rate for different beam sizes. In this case, the strain rate $10^{-2}/s$ was applied to all beam sizes, 1, 2, and 3 as listed in Table 2. This case is to show the effect of beam size on fracture properties of RAC beams.

Maximum forces obtained from the numerical simulations can be compared to those from the experiments (Musiket et al. 2016). The forces from the experiments that will be compared to the simulation results are shown as red dot-ellipses in Table 4. The load and Crack Mouth Opening Displacement (Force-CMOD) curves, crack propagation and stress distribution during crack development were also obtained. Computational time is about 45 min for each simulation. The simulations, in some cases especially for higher strain rates, were terminated after the peak loads were obtained due to the convergence difficulty.

Tables 5 and 6 show the comparisons of the simulated ultimate loads and test data for the two cases. It can be seen that the simulation results agreed with test data quite well in Table 5 and not as well in Table 6. The reasons will be discussed later. Figure 8 shows damaged elements (red) and crack-initiated elements (green) during crack propagation processes. Figures 9 and 10 show the full Force versus CMOD curves and Von Mises stress contours at both peak load and final deformed stage for Case 1 and 2, respectively.

For Case 1: Fixed beam size under different loading rates. As seen in the three stress contours on the left of Fig. 9a, the effect of strain rate on stress distribution and crack propagation is obvious. The higher the strain rates, the wider the high stresses spread in the crack propagation zone. This results help to explain that the effective fracture process zone size, c_f, increases with increasing loading rate, which was reported by Musiket et al. (2016) in their experimental study. In Fig. 9b, the maximum forces from numerical results are in good agreement with experiment results. The post-peak Force versus CMOD curves from the simulation follow the same trend of the test data. This means that the two new material models used in the numerical simulation can characterize the effect of high loading rate on RAC very well.

For Case 2: Fixed loading rate for different beam sizes. The results of numerical simulations for case 2 are shown in Fig. 10. In this case, the post-peak Force versus CMOD curves from the simulation follow the same trend of the test data. The stress distributions in the beams of different sizes are similar. However, comparing with the numerical results of Case 1, the peak loads from the simulations of Case 2 do not match very well with the experimental results. The differences between those maximum forces for different sizes of beams are 32.4, 14.5, and − 7.6 %, respectively. From Fig. 10b, one can see that the maximum force from the simulation increases with increasing beam size. Since the beams double their sizes from size 1 to size 2 and from size 2 to size 3 (See Table 2), the maximum loads from the simulation also double, the same as the beam size. On the other hand, the experimental results do not follow the same linear relation. This is due to the fact that the maximum forces of RAC notched beams follow the size-effect law (Bazant 1984), which were evidenced and discussed in detail for the experimental results (Musiket et al. 2016). The size effect for RAC beams was not considered in the fracture criteria adopted in ABAQUS^R and not in the two new material models. This will be a topic for future research.

7 Conclusions

Fracture tests of recycled aggregate concrete (RAC) beams of different sizes were conducted under high loading rates. In order to characterize the effect of high loading rate on the behavior of RAC beams, two new material models were used together with the commercial finite element software ABAQUS^R.

One of the two new material models is a viscoelastic model that can predict the increase of stiffness (modulus of elasticity) of RAC with increasing loading rate, and the other one is a multiphase composite model that can determine the effective stiffness of RAC taking into account the special internal structure of recycled aggregate, such as the residual cement paste on the natural aggregate core. Combining the two new material models, the stiffness of RAC under high loading rate can be estimated.

Two different cases were considered in the numerical simulation. Case 1 is for fixed beam size under different loading rates, which can show the effect of loading rate on fracture properties of RAC beams. Case 2 is for fixed loading rate with different beam sizes, which can show the effect of beam size on fracture properties

of RAC beams. For both cases, the maximum load, full range Force-CMOD curve, and stress distributions at the maximum load and at the end of simulation were used to compare the simulation results and the test data.

For Case 1, the simulation results of the maximum loads under three different strain rates agreed with test data quite well. The Force-CMOD curves of the numerical simulation and test data showed similar trends. The higher the strain rates, the wider the high stresses spread in the crack propagation zone. This results help to explain that the effective fracture process zone size, c_f, increases with increasing loading rate. The good agreements with the test data indicated that the two new material models can characterize the effect of high loading rate on RAC beams very well.

For Case 2, the simulation results of the maximum loads of three beams of different sizes under a fixed strain rate of $10^{-2}/s$ agreed with test data not as well as those of Case 1. The post-peak Force versus CMOD curves from the simulation follow the same trend of the test data. The stress distributions in the beams of different sizes are similar. On the other hand, the maximum loads predicted by the numerical model did not agree very well with test data. This is due to the fact that the maximum forces of RAC notched beams follow the size-effect law as indicted in the test data. The size effect for RAC beams was not considered in the fracture criteria adopted in ABAQUS^R and not in the two new material models. This will be a topic for future research.

Acknowledgements The authors wish to acknowledge the partial support by the US National Science Foundation under Grant CMMI-0900607 to University of Colorado at Boulder. Opinions expressed in this paper are those of the authors and do not necessarily reflect those of the sponsor.

References

Barker DB, Hawkins NM, Jeang FL, Cho KZ, Kobayashi AS (1985) Concrete fracture in CLWL specimen. J Eng Mech ASCE 111(5):623–638

Bazant ZP (1984) Size effect in blunt fracture: concrete, rock, metal. Eng Mech 110:518–535

Bazant ZP, Oh BH (1983) Crack band theory for fracture of concrete. Mater Struct 16(93):155–177

Bazant ZP, Xi Y (1995) Continuous Retardation spectrum for solidification theory of concrete creep. J Eng Mech ASCE 121(2):281–288

Elices M, Rocco C, Rosello C (2009) Cohesive crack modeling of a simple concrete: experimental and numerical results. Eng Fract Mech 76:1398–1410

Ghosh S, Lee K, Raghavan P (2001) A multi-level computational model for multi-scale damage analysis in composite and porous materials. Int J Solids Struct 38:2335–2385

Hillerborg A, Modeer M, Petersson PE (1976) Analysis of crack formation and crack growth in concrete by means of fracture mechanics and finite elements. Cem Concr Res 6:773–782

Jenq YS, Shah SP (1985) Two parameter fracture model for concrete. J Eng Mech ASCE 111(10):1227–1241

Liang Y, Ye Z, Vernerey F, Xi Y (2013) Development of processing methods to improve strength of concrete with 100% recycled coarse aggregate. J Mater Civ Eng ASCE. doi:10.1061/(ASCE)MT.1943-5533.0000909

Moës N, Dolbow J, Belytschko T (1999) A finite element method for crack growth without remeshing. Int J Numer Methods Eng 46:131–150

Musiket K (2014) Mechanical properties of recycled aggregate concrete under different loading rates, Ph.D. Dissertation, University of Colorado at Boulder, Boulder

Musiket K, Rosendahl M, Xi Y (2016) Fracture of recycled aggregate concrete under high loading rates. J Mater Civil Eng ASCE. doi:10.1061/(ASCE)MT.1943-5533.0001513

Nallathambi P, Karihaloo BL (1986) Determination of specimen-size independent fracture toughness of plain concrete. Mag Concr Res 38(135):67–76

Rabczuk T, Song J-H, Belytschko T (2009) Simulations of instability in dynamic fracture by the cracking particles method. Eng Fract Mech 76(6):730–741

Rabczuk T, Zi G, Bordas S, Hung N-X (2010) A simple and robust three-dimensional cracking-particle method without enrichment. Comput Methods Appl Mech Eng 199(37–40):2437–2455

Rabczuk T, Belytschko T (2007) A three-dimensional large deformation mechfree method for arbitraty evolving cracks. Comput Methods Appl Mech Eng 196(29–30):2777–2799

Rabczuk T, Eibl J (2003) Simulation of high velocity concrete fragmentation using SPH/MLSPH. Int J Numer Meth Eng 56(10):1421–1444

Rabczuk T, Eibl J (2006) Modelling dynamic failure of concrete with meshfree methods. Int J Impact Eng 32(11):1878–1897

Raghavan P, Ghosh S (2007) Concurrent multi-scale analysis of elastic composites by a multi-level computational model. Comput Method Appl Mech Eng 193:497–538

Roesler J, Paulino GH, Park K, Gaedicke C (2007) Concrete fracture prediction using bilinear softening. Cem Concr Res 29:300–312

Song JH, Areias PMA, Belytschko T (2006) A method for dynamic crack and shear band propagation with phantom nodes. Int J Numer Meth Eng 67:868–893

Vernerey F, Liu WK, Moran B, Olson GB (2008a) A micromorphic model for the multiple scale failure of heterogeneous materials. J Mech Phys Solids 56(4):1320–1347

Vernerey F, Liu WK, Moran B, Olson GB (2008b) Multi-length scale micromorphic process zone model. Comput Mech 44(3):433–445

Vernerey F, Kabiri M (2014a) An adaptive concurrent multiscale method for microstructured elastic solids. Comput Methods Appl Mech Eng 241:52–64

Vernerey F, Kabiri M (2014b) Adaptive concurrent multiscale model for fracture and crack propagation in heterogeneous media. Comput Methods Appl Mech Eng 276:566–588

Wagner GJ, Liu WK (2003) Coupling of atomistic and continuum simulations using a bridging scale decomposition. Comput Mater Sci 190:249–274

Xi Y, Jennings HM (1997) Shrinkage of cement paste and concrete modeled by a multiscale effective homogeneous theory. Mater Struct (RILEM) 30:329–339

Xu S, Reinhardt HW (1998) Crack extension resistance and fracture properties of quasibrittle materials like concrete based on the complete process of fracture. Int J Fract 92:71–99

Zhao Y, Xu S, Wu Z (2007) Variation of fracture energy dissipation along evolving fracture process zones in concrete. J Mater Civil Eng ASCE 19(8):625–633

Zhuang X, Cai Y, Augarde C (2014) A meshless sub-region radial point interpolation method for accurate calculation of crack tip fields. Theoret Appl Fract Mech 69:118–125